Available online at www.sciencedirect.com
SCIENCE DIRECT
International Journal of Mass Spectrometry 252 (2006) 79–95
International Journal of Mass Spectrometry
www.elsevier.com/locate/ijms

The frequency factor in statistical fullerene decay

K. Hansen [a,*], E.E.B. Campbell [a], O. Echt [b]

[a] Department of Physics, Göteborg University, SE-41296 Gothenburg, Sweden
[b] Department of Physics, University of New Hampshire, Durham, NH 03824, USA

Received 11 January 2006; received in revised form 18 January 2006; accepted 18 January 2006
Available online 24 March 2006

Abstract

Experiments on fullerene decay are reviewed and the frequency factor for C_2 emission is extracted. The value is also calculated theoretically. Inclusion of a number of previously disregarded degrees of freedom for the products increase the theoretical estimate for C_{60} to above 10^{20} s^{-1}, in good agreement with experimental results.

Keywords: Fullerene; Unimolecular decay

1. Introduction

It is a remarkable fact that the fullerenes, despite being intensively studied during the two decades that have passed since their discovery [1], have important properties that have only recently been understood. The geometric structure of these all-carbon molecules, based on pentagons and hexagons, was established unambiguously [2,3] soon after the discovery of a method to produce the molecules in bulk quantities [3], as were a number of other properties, including those associated with the solid state [4]. Gas-phase properties proved more elusive, in particular those associated with unimolecular decay of the fullerenes. Free positively charged fullerenes decay by emission of C_2 and electromagnetic radiation, and for the neutrals and anions also by electron emission [5–15]. The nature of delayed electron emission has been a matter of discussion [12,16–20] but it now appears most likely that all these processes are of statistical nature at timescales of μs and longer [21–27]. Presently, only the delayed ionization data of [19], obtained with far infrared excitation, seem to contradict the generality of this conclusion. Hopefully more experiments with this mode of excitation will shed new light on the issue.

On the timescale of tens of μs, the three decay channels occur in parallel, making fullerenes, if not the only molecule for which this happens, at least the most well documented. The emission of both electrons and atomic fragments can be efficiently described with a few parameters only, an activation energy, a frequency factor, and the energy content of the molecule, in addition to the caloric curve which relates excitation energy and temperature. The purpose of this paper is to summarize experimental results which can be used to extract the frequency factor, also called the *A*-factor, and to provide a theoretical calculation of the same quantity.

Both of these tasks are less than straightforward. The experimental determination of the frequency factor suffers from an effect that can be traced back to the relatively large number of degrees of freedom in the molecules in combination with the high stability against disintegration. These two factors have the effect that the excitation energy required to induce fragmentation on the μs timescale, say, is much larger than the activation energy. In chemical physics this difference in energies is known as the kinetic shift. Measurements of the so-called breakdown curves give values of 40–50 eV for the appearance of fragments of C_{60}^+ [28]. Although such energies can certainly be deposited into the molecules, as witnessed by the many experiments, e.g., on photo fragmentation of fullerenes, it poses serious problems when one wants to control the amount of excitation energy. These problems are particularly relevant for an Arrhenius analysis, which would otherwise be an efficient tool to extract activation energies and frequency factors. A classical Arrhenius analysis is based on experimental data pertaining to a canonical ensemble, but it can also be made for a microcanonical ensemble. The latter, involving molecular beam experiments, allows measurements of rate constants down to μs timescales.

* Corresponding author.
E-mail address: klavs@physics.gu.se (K. Hansen).

1387-3806/$ – see front matter © 2006 Elsevier B.V. All rights reserved.
doi:10.1016/j.ijms.2006.01.052

Nomenclature

c	heat capacity (canonical, and generic)
c_m	microcanonical heat capacity (see Eq. (6))
D	dissociation energy, activation energy for C_2 loss. Subscript N refers to fullerene of size N, superscript + to C_N^+
E	excitation energy of molecule
E_a	activation energy (generic, see Eq. (1))
$f(E)$	distribution function
F	Helmholtz free energy of the electronic subsystem. Subscripts 0 and + refer to neutral and charged molecule
g	electronic degeneracy of the molecule or electron. Subscripts 0 and + refer to neutral and charged molecule
$g(E)$	distribution function
G_N	isomer degeneracy of size N
I_e	electron emission rate
k	rate constant, generic. Subscripts a and e refer to emission of C_2 and electron, respectively
p	exponent in powerlaw (Eq. (14))
T	temperature (canonical, and generic)
T_e	emission temperature (see Eq. (5))
T_f	fragment temperature (see Eq. (7))
$V(r)$	potential at the point of no return (max of centrifugal barrier)
ω_v	vibrational frequency
Y_e	total electron yield (see Eq. (16))

Greek letters

Φ	ionization energy (generic) (subscript n refers to fullerene of size n)
ε	total kinetic energy release (KER) in center-of-mass
ρ	level density. Subscripts 0 and + refer to neutral and charged molecule, respectively. Subscript v refers to nuclear degrees of freedom
σ_E	standard deviation of excitation energy distribution
$\sigma(\varepsilon)$	cross section for electron capture
ω	Arrhenius factor (generic, see Eq. (1)). Subscript a refers to C_2 loss, subscript e refers to electron emission

The analysis is analogous to that of the canonical case, apart from the application of the finite heat bath correction, discussed elsewhere.

Unfortunately, the requirements on the width of the excitation energy distribution are rather severe if one wants to perform an Arrhenius analysis of a microcanonical ensemble. To be able to assign a single decay rate constant to the ensemble with an average excitation energy $\langle E \rangle$ and a width σ_E one may use the criterion that the natural logarithm of the rate constant should vary by less than one over the distribution. If this is the case, the decay will follow a simple exponential decay, and the rate constant can be determined unambiguously. This requires that the relative energy width is less than a few percent of the total excitation energy. For the 40–50 eV quoted previously for C_{60}, this upper limit on the width corresponds to about 1.5 eV, which is close to $2\sigma_E$ in a thermal population from a source where the molecule is sublimed at 400 °C. Any additional width imparted by the additional 35–45 eV needed to cause measurable decay will then exceed the critical value. This will give rise to decays that have a powerlaw time dependence, without any characteristic timescale. Although this situation does not allow one to extract rate constants from experimental data, it may nevertheless contain useful information about the decay. This point will be discussed in detail below.

The origin of the width in energy is the size of the molecule. The relatively large number of vibrational degrees of freedom with low energy quanta will give rise to a large heat capacity even at the moderate source temperatures. This situation should be contrasted with the one prevailing for small molecules, where a lower source temperature and vibrations higher in frequency and smaller in number make it possible to have a vibrational energy distribution which is in the worst case a sum of a few delta functions. Several researchers have, indeed, interpreted their spectra pertaining to delayed electron emission from free fullerenes by a superposition of two or three distinct rate constants [12,16,17,29]. (Probing the *dissociation* of multi-photon-excited neutral fullerenes and its time dependence has not yet been possible.) However, the significance of the reported rate constants has remained obscure. Experimental data from multiple photon absorption are generally not of the single exponential type and require a fit with several rate constants. It is not possible to assign the fitted rate constants to a set of specific numbers of photons absorbed, because the values of these fitted numbers do not increase with photon energy. Neither do the fitted rate constants increase with source temperature, as they should for an effusive source.

The limited range of timescales often used in experiments on fullerene ions poses another but related problem. Although the use of ion traps or storage rings can greatly expand the available time range, there are nevertheless important limitations. The smallest time is limited to roughly a μs. The longest time is not instrumental, in which case it would be seconds or even longer. Fullerenes emit electromagnetic thermal radiation, akin to black body radiation, but with a slightly stronger dependence on the temperature than the Planck radiation [21,30]. Still, this temperature dependence of the emitted radiative power is much weaker than for thermally activated processes (i.e., electron and C_2 emission) which vary exponentially with the inverse temperature. At high temperature, C_2 emission is the primary decay channel whereas energy is lost predominantly by thermal radiation at low temperatures. The cross-over temperature corresponds to a C_2 emission rate constant from 10^4 to 10^5 s^{-1} [13]; the precise value depending on the parent molecule. Hence there is a limitation on the dynamic range of about a factor of 100, partly intrinsic to the molecules and partly instrumental. This limitation on the timescale reduces strongly the temperature interval, and equivalently the energy window, which carries useful information in

experiments on C_2 decay of ions. As a rule of thumb one has an increase of a factor of 20 in rate constants when the energy is increased by 10% on the observational timescale of μs, and the time range covered thus corresponds to a mere 15% difference in energy. A simultaneous determination of the frequency factor and the dissociation energy is very difficult under these conditions. It corresponds to taking a derivative at an ill-defined value of the argument. These difficulties are closely related to those associated with the Arrhenius analysis.

With these difficulties in mind one may instead attempt a frontal attack with the Arrhenius expression, extracting the frequency factor from a single well-known excitation energy, possibly a mean energy. This is only possible if one knows the dissociation energy as well as the caloric curve linking E and T. Traditionally, the dissociation energy, D, has been the desired quantity and to obtain this, one has assumed a value of the frequency factor. As will be shown later, an error in this frequency factor will be correlated with the resulting error in the dissociation energy extracted from the experiments, which will be incorrect by the term $k_B T \ln(\alpha)$, where α is the ratio of the correct frequency factor to the erroneous one. A wide range of frequency factors has been reported in the literature, spanning orders of magnitude. The logarithmic dependence on the error in the frequency factor explains why these values can still be compatible with physically reasonable values of D. Thus the frequency factors extracted from a number of experiments are closely related to the determination of the dissociation energies.

A number of different assumptions must be made in the calculation of the frequency factor. Most workers in the field of unimolecular decay, including fullerene decay, use the transition state formulation known as RRKM [31]. The method applies the concept of a reaction coordinate and calculates the rate constant as the relative population at the top of the potential along this coordinate, multiplied by a flux and a phase space factor. This formalism has obvious advantages when dealing with molecules where steric factors impose strong restrictions on the possible geometries of reacting species. This is not the case for so-called 'orbiting transition states' where no steric factors are present, a situation which seems to be realized in highly excited fullerenes. For this type of reaction, decay can be described in a transparent way with an alternative formulation of rate theory, detailed balance, which is used extensively in nuclear physics and which has found some application in cluster science [32–34]. It relates the populations of parent and product states to the statistical weight of these species, and calculates the decay rate constant in terms of the rate constant for the inverse process. The crucial point is that the latter is easily calculated for an orbiting transition state. The assumptions necessary to apply detailed balance are similar to those needed for RRKM theory (assumptions about the transition state in the latter correspond to those for the cross section in the former). Likewise, two level densities need to be estimated, viz. those for the parent and the product/transition state. The advantage of detailed balance in this connection is that the two level densities can be calculated by reference to the asymptotically free species, and that renders the calculation more transparent.

The remainder of the paper will be divided into two parts, one which reviews critically the available experimental evidence, and one where the theoretical best estimate of the frequency factor is presented. In spite of the experimental difficulties mentioned above, it is nevertheless possible to make a number of independent estimates for the frequency factor. The estimates will be seen to agree reasonably well with the theoretical estimate.

2. Some basic relations

In thermal equilibrium, the rate constant of a reaction with activation energy E_a may be expressed by the Arrhenius relation,

$$k(T) = \omega \exp\left(-\frac{E_a}{k_B T}\right). \tag{1}$$

Although the pre-exponential factor ω, aka Arrhenius factor or A-factor, is not independent of T, the overwhelming temperature dependence of k arises from the exponential factor. A measurement of k versus T therefore provides values for both ω and E_a. For quite a while it was assumed that all atomic clusters, including the fullerenes, are characterized by about the same frequency factor for monomer loss, $\omega_a \approx 1.6 \times 10^{15}\,\mathrm{s}^{-1}$ [35], and the object of scientific desire, D, then would seem to follow from just a single measurement of k for some value of the excitation energy E.

Measurements of C_2 emission from C_{60} in true thermal equilibrium are not easy and most measurements have been made on unimolecular dissociation in vacuum,

$$C_{60} \rightarrow C_{58} + C_2. \tag{2}$$

Many published gas-phase experiments involve the cation instead of the neutral molecule:

$$C_{60}^+ \rightarrow C_{58}^+ + C_2. \tag{3}$$

We will denote the activation energies for reactions (2) and (3) by D_N and D_N^+, respectively, where N indicates the size of the fullerene, and use E_a for a generic activation energy. These quantities are linked by a thermodynamical cycle,

$$D_{60} + \Phi_{58} = D_{60}^+ + \Phi_{60} \tag{4}$$

where Φ_N denotes the adiabatic ionization energy of the fullerene C_N. Φ_{60} and Φ_{58} are known quite well from charge transfer and single-photon-ionization data [36–38]. The generally accepted value for $\Phi_{60} - \Phi_{58}$ is 0.54 ± 0.10 eV.

The rate constant for unimolecular dissociation in vacuum may be described by an Arrhenius relation if one properly defines the temperature of a small, isolated system that carries a vibrational excitation energy E. A transparent description is provided by the concept of the microcanonical temperature [39,40]. If the excitation energy of the parent is E and its microcanonical temperature is T_m then, to first order in $1/c_m$, the so-called emission temperature to be used in Eq. (1) is:

$$T_e = T_m - \frac{E_a}{2c_m}. \tag{5}$$

c_m is the derivative of E with respect to the microcanonical temperature T_m, i.e., c_m is the microcanonical heat capacity which is related to the canonical heat capacity c,

$$c_m \approx c - k_B. \tag{6}$$

c_m is often approximated by its high-temperature limit $(3N-7)k_B$, although it is not difficult to compute an accurate value from the vibrational frequencies of C_N. The second term in Eq. (5) is the finite heat bath correction [35,39]. Another relevant temperature is the fragment temperature T_f which is reflected in measurements of the kinetic energy release of the reaction. To first order one has:

$$T_f \approx T_e - \frac{E_a}{2c_m} \approx T_m - \frac{E_a}{c_m}. \tag{7}$$

3. Information and misinformation from Arrhenius plots

One of the difficulties associated with the determination of frequency factors in unimolecular decay is the experimentally feasible width of internal energy distributions, as mentioned in Section 1. The demand on the standard deviation of the energy σ_E can be calculated approximately if we use $\langle E\rangle \sim c_m T$ and an Arrhenius expression for k:

$$\delta\ \ln(k) = \frac{\mathrm{d}\ \ln(k)}{\mathrm{d}E} 2\sigma_E = \frac{D}{k_B T_e}\frac{2\sigma_E}{E} < 1, \tag{8}$$

where T_e is an effective emission temperature and we use $2\sigma_E$ to represent the width of the energy distribution. The special problem associated with large molecules is that a value of T_e which gives decay on an experimentally reasonable timescale involves a large energy, imparted by, e.g., a significant number of absorbed photons. An attempt to extract decay rate constants for a system with a width larger than the above is doomed to give too small a variation with energy, and hence to produce an Arrhenius plot with too low a slope. One clear example of this (for electron emission from anions) is found in [41] and discussed in [21]. As of today, no experiment on thermally activated decomposition of C_{60} or C_{60}^+ has been reported in which the fullerenes constituted a microcanonical ensemble to a reasonably good approximation.

The experiment of Ding and co-workers, who applied one-photon-ionization in the energy range 15–120 eV combined with threshold-photoelectron-photoion coincidence (TPEPICO) to gas-phase fullerenes [42] would have qualified if successful. A more recent, non-coincidence one-photon study [43] suggests that TPEPICO should be given another chance.

Experiments with insertion of a metal ion into the fullerene cage to form endohedrals are also potentially useful [44–46]. In this approach, the excitation energy E is simply the collision energy, plus the initial thermal energy of C_N and the (poorly known but rather small) adiabatic binding energy between Na^+ and C_N.

Most of the experiments that potentially contain the problem with broad energy distributions, or which have been interpreted with an assumed frequency factor, have been performed at timescales from microseconds to milliseconds [44,47–54].

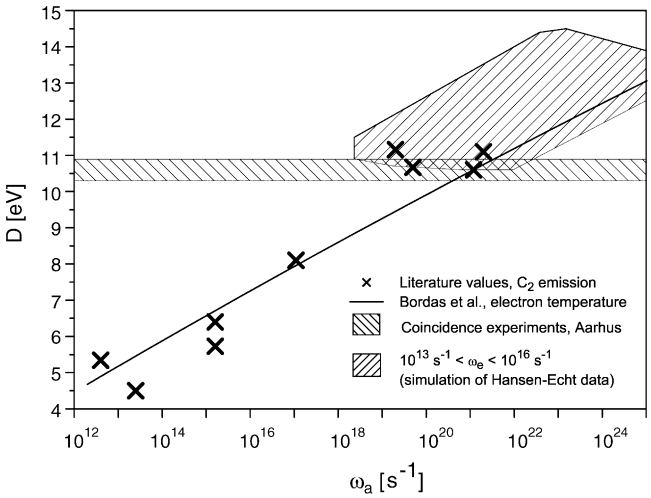

Fig. 1. Simulation of the data from [64] and literature values of determinations of sets of (D, ω_a) for C_{60} as described in the text. Crosses refer to experimental values. They are from (in order of increasing frequency factor) [48,49,47,54,52,51,44,53,50]. The horizontal lines are the dissociation energy ± one standard deviation from the Aarhus coincidence experiments [53].

These experiments give widely varying values of the frequency factor. The frequency factor and dissociation energy extracted from such data will be correlated which can be seen by considering the timescales involved. Compared with the reciprocal frequency factor, a microsecond is a very long time, and to a first approximation one can set all the experimental timescales equal. If the value of the frequency factor is assumed incorrectly to be $\alpha\omega_a$, where α is a dimensionless number, the error in the dissociation energy, D, can be estimated with the simple rewrite:

$$k = \omega_a \mathrm{e}^{-D/k_B T_e} = \alpha\omega_a \mathrm{e}^{-(D+k_B T_e\ \ln(\alpha))/k_B T_e} = \omega_a' \mathrm{e}^{-D'/k_B T_e}. \tag{9}$$

from which we obtain the error of $D' - D = k_B T_e \ln(\alpha)$ in D. On μs timescales the ratio of the activation energy D to the temperature times k_B is expected to be 30–35 for $\omega_a = 10^{19}$ to $10^{21}\ \mathrm{s}^{-1}$, and it varies only slowly with the timescale. A plot of D' versus $\ln(\omega_a')$ will thus give a universal curve with slope $k_B T_e$ and intercept $-k_B T_e \ln(1\ \mu\mathrm{s})$, and a reduction of the possible values of D and $\ln(\omega_a)$ to those on the line. The published data from [44,47–54] are plotted in Fig. 1 together with other data to be discussed below. The data points shown do indeed have the expected correlation. The temperature can be extracted from the slope and intercept of the straight line. The two different procedures yield temperatures of 4100 K and 4800 K which are, everything considered, in surprisingly good agreement with the expected temperatures of 3000–4000 K.

4. Breakdown curves

A number of experiments have been performed in order to construct the breakdown curves, which show the survival probability of ions as a function of their excitation energy [28,52,55,56]. This method requires a connection between E and

directly controlled experimental parameters such as the electron energy in electron impact experiments, or the collision energy in surface collision experiments. Several experiments have been reported in which the energy deposition function was determined. Electron impact ionization, in particular, has been useful because of the well-defined upper cut-off in the energy distribution. For C_{60}^+ produced from a thermal beam of C_{60} the cut-off is $E_{el} - \Phi_{60} + E(T_{ov})$ where E_{el} is the electron impact energy, $\Phi_{60} = 7.6$ eV the ionization energy of C_{60}, and $E(T_{ov})$ the thermal energy of C_{60} vaporized at temperature T_{ov} (assumed to be low enough so thermal decomposition and radiative cooling of the neutral beam are negligible). In the experiments, C_{60}^+ forms already at the threshold for direct ionization, $E_{el} = 7.6$ eV, but C_{58}^+ fragment ions do not appear until the electron energy reaches about 45 eV. Smaller fragment ions appear at even higher energies. The exact values of the appearance energies depend on the observation time and the thermal energy $E(T_{ov})$. The observations are consistent with statistical formation of fragment ions by sequential loss of C_2 from hot C_{60}^+. Dissociation energies derived from these and similar experiments [57] are commensurable with the value of the pre-exponential factor for C_2 loss that was assumed in the data analysis. The conclusion is that even if the energy deposition function is known in these experiments, the value of the frequency factor can only be determined from these experiments if the dissociation energy is entered into the data analysis or vice versa.

5. Kinetic energy release distributions

Electron impact ionization, used to measure the breakdown curves, has the advantage of a sharply defined upper limit but it produces no distinct lower limit. Most excitation mechanisms, such as surface collisions [57–63] and multiphoton excitation [12,16,64–66], also give rise to very broad energy distributions. Cooling by evaporation, though, will always introduce an upper cut-off. Moreover, those molecules that are only weakly excited will not contribute to the reaction because the probability for decay is $1 - \exp(-kt)$. Taken together, the energy distribution of molecules that contribute to the decay signal observed at time t is, in the absence of competing decay channels, centered at an energy E that approximately corresponds to a rate constant of $1/t$.

This self-selective mechanism has been applied widely in attempts to determine the dissociation energy for C_2 loss from empty and filled (that is, endohedral) fullerene cations [47,50,51,67–73] through measurements of the kinetic energy release functions.

For statistical processes, the distribution $f(\varepsilon)$ of kinetic energy, ε, reveals the microcanonical temperature T_f of the fragment [34,39,74,75]:

$$f(\varepsilon) \propto \varepsilon\sigma(\varepsilon) \exp\left(-\frac{\varepsilon}{k_B T_f}\right) \tag{10}$$

where $\sigma(\varepsilon)$ is the capture cross section for the reverse reaction, and ε is summed over all products. If the reaction produces only two products, such as reactions (2) and (3), then a measurement of the energy distribution of one of them will provide $f(\varepsilon)$ and, hence, T_f and T_m.

One issue that limits the accuracy of the method is the rather long measurement time t. For fullerene ions, radiative cooling cannot be ignored if $t \gg 10\,\mu$s [13,76]. But the two main problems in connection with frequency factors or dissociation energies are that (1) the inversion of experimental data to extract a temperature demands that the cross section is known [34,39,47,72,77], and (2) even if the energy content of a molecule is determined in the form of a microcanonical temperature, it still requires either the dissociation energy or the frequency factor to be known to extract the other.

Although these problems make absolute determinations of frequency factors with the method doubtful, the kinetic energy distributions are nevertheless interesting in their own right because they provide estimates of the magnitude of T_f to better than approximately 20%.

The value of the average kinetic energy release, $\bar{\varepsilon}$, is $2k_BT_f$ for an C_2 capture cross section which is independent of the fragment kinetic energy, e.g., a geometric cross section. This arises as the mean of the distribution $\varepsilon \exp(\varepsilon/k_BT_f)$. Experiments on positively charged fullerenes give consistently distributions of the form $\sqrt{\varepsilon}\exp(-\varepsilon/k_BT_f)$, which has a mean value of $\bar{\varepsilon} = 1.5k_BT_f$ [51,78]. The reduction from 2 to 1.5 is now well understood as the consequence of the long range interactions between the polarizable C_2 and the charged C_{N-2}^+ [77], or in general as interactions involving polarizabilies [72], which gives rise to a Langevin-like capture cross section. The cross-over from an energy independent cross section to a Langevin-like cross section is determined by the ratio of the polarization energy at the capture distance and the temperature [77]; at values below unity the capture is essentially Langevin-like, and energy independent above unity. We must expect a higher coefficient for k_BT_f for $\bar{\varepsilon}$, between 1.5 and 2, for the decay of the neutral species.

Although the kinetic energy distributions are indistinguishable from those arising from a Langevin cross section, the analysis in both [77] and [72] shows that this similarity can be misleading and lead to an overestimate of T_f by as much as 20%. Interestingly, this number is close to the discrepancy, 18%, between the experimental T_f from [51] and those expected from an analysis of the electron emission data of Bordas and co-workers [23,26,27] that will be discussed elsewhere in the paper. If this holds, it may give an experimental value for the polarizability of C_2 which has not previously been measured experimentally. The two, very different, theoretical values are, spherically averaged, 78 a_0^3 [79] and 27 and 24 a_0^3 [80]. From the data in [51] and assuming that the C_2 is captured when it reaches a distance of 3.5 Å from the center of the C_{58}^+ one gets a polarizability between 1.7 Å^3 and 2.9 Å^3, i.e., significantly lower. A discussion of these interesting questions will take us too far astray.

The conclusion of this discussion of KER data is that measured KER data alone are not sufficient to determine temperatures to better than 10–20% even if they have a very low intrinsic statistical uncertainty, although the method suggested in [51] seems promising. In addition, it is still only with the input of a known dissociation energy this type of data can be used to extract

the frequency factor. In calculations of corrections we will use the approximate temperature dependence $\bar{\varepsilon} = 1.5k_BT_f$.

6. Time matters, and why competition is good for you

None of the experiments discussed above has separately provided values for the dissociation energy (either D_{60} or D_{60}^+) and the Arrhenius factor ω_a.

A decade ago it was realized that more information can be garnered if another dimension, time, is included in the analysis. The value of these experiments is two-fold: (i) they can reveal the presence of elusive channels that are difficult to track otherwise, and (ii) they can be used to unambiguously determine key quantities, such as the emissivity for black body radiation [5,13,55,81], or the activation energy for C_2 loss [24,53,64,76,82].

The competition between C_2 loss and thermal radiation has been described shortly elsewhere in the paper and here we focus on the competition between electron emission (thermionic emission) and dissociation (C_2 loss) from neutral fullerenes. Both reactions can be described by Arrhenius relations, and the two reactions combined provided early evidence that the frequency factor for C_2 emission, ω_a, greatly exceeds the Klots value of $\omega_a \approx 1.6 \times 10^{15}\,\mathrm{s}^{-1}$ [35].

Let us consider an ensemble of C_{60} molecules that was initially prepared with an energy distribution $g(E)$. If only one reaction (with a rate constant $k(E)$) is possible, then the rate constant averaged over the ensemble at time t will be:

$$\bar{k}(t) = \int_0^\infty k(E)g(E)\mathrm{e}^{-kt}\,\mathrm{d}E. \tag{11}$$

We have assumed that the ensemble is not populated by decay of larger molecules. If $g(E)$ does not vary stronger than, e.g., a small power of the energy over the energy range that supports decay at time t, one readily obtains from Eq. (11):

$$\bar{k} \propto t^{-1}. \tag{12}$$

This is indeed observed in storage ring experiments with decay of small metal cluster anions, and in similar experiments with (the short time) decay of fullerene anions [5,83]. An energy distribution that is not flat will only slightly modify this time dependence, as shown in Appendix A.

Things get more interesting if two channels compete. If the electron emission (rate k_e) is being monitored in the presence of C_2 emission (rate k_a), one obtains the emission intensity:

$$I_e(t) = \int_0^\infty k_e(E)g(E)\mathrm{e}^{-(k_e+k_a)t}\,\mathrm{d}E. \tag{13}$$

With the assumption $k_e \ll k_a$, which is consistent with the results of a separate experiment which measured the total electron yield per C_{60} [65], one obtains:

$$I_e \propto t^{-p} \tag{14}$$

where

$$p \approx \frac{D}{\Phi}. \tag{15}$$

In Appendix A the corrections to this result from miscellaneous effects are discussed quantitatively. Here we merely mention that in the experiment a powerlaw was, indeed, observed, with an exponent $p = 0.64 \pm 0.10$ [64]. $\Phi_{60} = 7.6\,\mathrm{eV}$ then results in $D_{60} = 11.9 \pm 1.9\,\mathrm{eV}$. This result together with the assumption $k_e \ll k_a$ demands that ω_a exceeds ω_e by several orders of magnitude.

It is possible to get a first estimate of ω_a with simple arguments. The total electron yield was determined in [65] to a value of $Y_e = 2.6\%$. This value represents a lower limit in the sense that it only includes electrons produced within the retention time of the molecules in the active area of the detector, between zero and about $t_0 = 20\,\mu\mathrm{s}$. For an order of magnitude estimate the value of Y_e can be set equal to the ratio of rate constants:

$$Y_e \approx \frac{k_e}{k_a} = \frac{\omega_e \mathrm{e}^{-\Phi/k_BT_e}}{\omega_a \mathrm{e}^{-D/k_BT_e}}, \tag{16}$$

where we have neglected the correction due to different emission temperatures. The exponentials can be expressed as powers of each other, and with the identification $k_e = 1/t_{\mathrm{obs}}$, where t_{obs} is the reasonably well-defined measurement time, Eq. (16) is solved to yield:

$$\omega_a = Y_e^{D/\Phi}(\omega_e)^{D/\Phi}\frac{1}{t_{\mathrm{obs}}} = 9 \times 10^{22}\,\mathrm{s}^{-1}, \tag{17}$$

if the value $\omega_e = 8.3 \times 10^{14}\,\mathrm{s}^{-1}$ from Section 8 is used. As an estimate this cannot be an extremely reliable number, but it nevertheless shows that the frequency factors for electron emission and dimer emission are separated by a very large factor.

The above schematic calculation has been supplemented by a less transparent but more complete simulation of the data in [64], similar to the one performed in [84]. The electron emission rate constant was averaged over a flat energy distribution, stretching from 0 K to 10,000 K, with a numerical resolution of $\mathrm{d}T = 2\,\mathrm{K}$. The highest temperature, $T_{\max}$, corresponds to approximately 150 eV internal energy for neutral C_{60}, far beyond the value required for decay on the nanosecond timescale. The electron emission rate, I_e, was calculated for three different times, 0.1 μs, 1 μs and 10 μs, as:

$$I_e(t) = \frac{\int_0^{T_{\max}} k_e(T)\mathrm{e}^{-(k_e+k_a)t}\,\mathrm{d}T}{\int_0^{T_{\max}} \mathrm{d}T}. \tag{18}$$

The exponential factor accounts for the depletion at time t. The expressions used for k_e and k_a were:

$$k_e = \omega_e \exp\left(-\frac{\Phi}{k_BT - k_B\Phi/2c_m}\right),$$

$$k_a = \omega_a \exp\left(-\frac{D}{k_BT - k_BD/2c_m}\right), \tag{19}$$

with $\Phi = 7.6\,\mathrm{eV}$ the ionization potential of C_{60}. The parameterization of the two rate constants include the finite heat bath correction explicitly, but are otherwise kept simple on purpose, in order to have as transparent an expression as possible.

Both frequency factors were varied between $10^3\,\mathrm{s}^{-1}$ and $10^{27}\,\mathrm{s}^{-1}$ with steps of factors of 2, and the dissociation energy in

the interval 2 eV $\leq D \leq$ 15 eV, with steps of 0.1 eV. Three criteria were used for agreement with experiments. First of all, the value of p was restricted to $0.55 \leq p \leq 0.75$. The limits were decided to take both experimental and estimated systematic uncertainties into account. Second, the curvature of the log–log plot should not deviate appreciably from zero. Quantitatively, the absolute difference between the two slopes determined from the rates at 0.1 μs and 1 μs, and at 1 μs and 10 μs, were restricted to be less than 0.03, i.e., ca. 5% of the mean value. The third criterion was a total electron yield which conforms with the measured limit of $Y_e \simeq 2.6\%$ used in the simple estimate above. This number depends somewhat on the precise photon absorption statistics in the experiments and the interval chosen in the simulation. For this reason fairly generous limits were chosen, $0.005 \leq Y_e \leq 0.2$.

In addition to the explicit inclusion of the finite heat bath corrections to the rate constants the simulations thus also automatically include the correction of order $1/\ln(\omega_a t)$ to p which was pointed out by Klots (see Eq. (17) in [85]). It does not include any temperature dependence of the frequency factors. It is also restricted to a flat initial energy distribution.

The simulation results are shown in Fig. 1. All sets of ω_e, ω_a values that fulfill the three conditions are contained in the hatched area, with the restriction that the electron emission frequency factor be between $10^{13}\,s^{-1}$ and $10^{16}\,s^{-1}$. Values beyond these are found to the left ($\omega_e < 10^{13}\,s^{-1}$) and right ($\omega_e > 10^{13}\,s^{-1}$) of the hatched area. The points show that a limited region of parameter space is consistent with the experimental results in [64], and that the lower edge overlaps with individual experimental points determined by others.

7. Metastable decay

Measurements of metastable decay fractions in molecular beams allow an independent probe of the frequency factor for charged particles. The number extracted is coupled to the heat capacity, as will be clear, but still gives estimates that are reliable enough to be interesting.

Metastable fractions are frequently measured in time-of-flight devices equipped with a reflectron, which is detuned from the optimal resolution so that molecules which have fragmented after the initial acceleration but before entry into the reflectron will appear as individual peaks which can be integrated and normalized to the total of parent and fragment peak. For the same conditions under which one observes a $1/t$ decay one will have a metastable fraction which grows with flight time as:

$$P \propto \int_{t_1}^{t_2} \frac{1}{t}\mathrm{d}t = \ln\left(\frac{t_2}{t_1}\right). \tag{20}$$

The constant of proportionality is calculated below.

The relationship hinges on the existence of a highest temperature, $T_{\max}$, in an ensemble of freely evaporating particles. This temperature can be derived from solving the relation:

$$k_a = \frac{1}{t} \tag{21}$$

with respect to the temperature:

$$T_{\max,N} = \frac{D_N}{2c_N} + \frac{D_N}{\ln(\omega_a t)}. \tag{22}$$

(c_N is the heat capacity). This relation already suggests why the frequency factor appears in the metastable fractions: $T_{\max,N}$ depends on time, albeit weakly, through the factor $1/\ln(\omega_a t)$.

A lowest temperature also exists, provided the molecules have evaporated at least once. Based on these observations it is possible to calculate the abundances in an ensemble of freely evaporating molecules to be [86]:

$$\begin{aligned} I_N &\propto c_N T_{\max,N} - c_{N+2} T_{\min,N} \\ &= \frac{D_N + D_{N+2}}{2} + \frac{D_N c_N - D_{N+2} c_{N+2}}{k_B \ln(\omega_a t)}, \end{aligned} \tag{23}$$

if the frequency factors for N and $N+2$ are assumed equal. Molecules, mass separated at time t_1 in the time-of-flight acceleration, will have a metastable decay fraction at t_2 of:

$$\begin{aligned} P(t_2, t_1) &= \frac{c_N(T_{\max,N}(t_1) - T_{\max,N}(t_2))}{I_N(t_1)} \\ &\approx \frac{c_N D_N}{k_B \ln(\omega_a t_1) \ln(\omega_a t_2) I_N(t_1)} \ln\left(\frac{t_2}{t_1}\right) \\ &= \frac{c_N D_N}{k_B \ln(\omega_a t_1) \ln(\omega_a t_2)(c_N T_{\max,N} - c_{N+2} T_{\min,N})} \\ &\quad \times \ln\left(\frac{t_2}{t_1}\right) \equiv \alpha_N \ln\left(\frac{t_2}{t_1}\right). \end{aligned} \tag{24}$$

A determination of $P(t_2, t_1)$ thus allows one to determine a combination of c_N, c_{N+2}, D_N, D_{N+2} and ω_a. The molecules cool not only by C_2 emission but also by emission of thermal radiation [13,81,82,87]. The presence of thermal radiation, however, only changes Eq. (24) by the addition of another term which depends on the difference $t_2 - t_1$. If this difference is kept constant in the experiments, the slope of P versus $\ln(t_2/t_1)$ is still given by Eq. (24). Radiative cooling also changes the value of t_2, which becomes equal to the cooling time, which is defined as the time it takes for the C_2 emission rate constant to decrease by a factor $1/e$. For cationic fullerenes it is on the order of several tens of μs, determined directly in the experiments [76]. For the purpose of this calculation we can then use the approximate value $\ln(\omega_a t_1)\ln(\omega_a t_2) \approx (\ln(\omega_a 10\,\mu s))^2$.

Together with experimentally determined slopes, α_N, we can use Eq. (24) and solve for $\ln(\omega_a 10\,\mu s)$ if we know the D_N's (and the c_N's). Instead of using D_N's from the literature, which may be influenced by assumed values of frequency factors, we rearrange Eq. (24) and sum over consecutive fullerene sizes in order to telescope the differences $c_N D_N - c_{N+2} D_{N+2}$ into the difference between the first and the last term in the sum. This cancels all terms $c_N D_N$ between the smallest and largest size in the measurement series. With the experimental slopes α_N the

procedure gives:

$$(\ln(\omega_a 10\,\mu s))^2 = \frac{\bar{D}\frac{\Delta N+2}{2} + \frac{1}{k_B \ln(\omega_a t_1)}(D_{N_{min}} c_{N_{min}} - D_{N_{max}} + 2c_{N_{max}+2})}{\sum \frac{c_N D_N}{k_B \alpha_N}}, \quad (25)$$

where $\bar{D}$ is the average dissociation energy over the range considered. The last term in the numerator can be approximated by setting the D_N's to the mean value, and we will use the same approximation for the denominator. In this term also the factor $\ln(\omega_a t_1)$ can be approximated with $\ln(\omega_a 10\,\mu s)$. Hence

$$(\ln(\omega_a 10\,\mu s))^2 \approx \frac{1 - (3/\ln(\omega_a 10\,\mu s))}{c_{\bar{N}} \overline{\alpha_N^{-1}}} \quad (26)$$

from which ω_a is easily found when the α_N's are known.

The derivation of Eq. (26) requires that the energy distribution over a mass is flat. This was not the case for the high statistics data in [14] due to limitations in the laser power. This is reflected in the mass abundance spectrum which decreases towards smaller fullerene masses. A correction to the radiative cooling parameter from this effect was calculated, based on the mass spectrum itself, with a procedure discussed in detail in [66]. A similar calculation for the frequency factor gives a correction of:

$$(\ln(\omega_a 10\,\mu s))^2 \rightarrow \frac{(\ln(\omega_a 10\,\mu s))^2}{1 - (\alpha' c_{\bar{N}}/(\ln(\omega_a 10\,\mu s))^2)\langle \ln(t_2/t_1)\rangle}. \quad (27)$$

The parameter α' is an experimental parameter on the order of $0.15/D$ to $0.3/D$, derived from the specific abundance spectra used and is thus not a universal parameter for fullerenes. The correction to $\ln(\omega_a 10\,\mu s)$ in Eq. (27) is typically 5%.

Experimental data from the parent molecules C_{60}, C_{70} and C_{84} were analyzed with the above formalism. If all frequency factors are identical the values should be identical for these three series (we have ignored the difference in mass separation time t_1 which is small on a logarithmic scale). The result is that for the range $N = 42$–58, the value is $\ln(\omega_a 10\,\mu s) = 34.1 \pm 1.2$, for $N = 52$–68 it is 32.2 ± 1.2, and for $N = 68$–82 it is 33.5 ± 2.2. These values are consistent with one single value of 33.2 ± 0.8. This analysis does not take into account the different degrees of radiative cooling, but these were found to be quite similar [14], and given the logarithmic dependence, small differences in cooling time will have very minor effects on the analysis.

Analogous numbers were extracted from the metastable decay of endohedral fullerenes, $La@C_N^+$, with $68 \leq N \leq 80$, produced by photoexcitation of $La@C_{82}$. The mean was $\ln(\omega_a 10\,\mu s) = 31.5 \pm 1.4$. The similarity with the empty fullerenes should not surprise; also the radiative cooling is quite similar [14].

In summary, the frequency factor is found from metastable fragmentation to be between $10^{19.1}\,s^{-1} \leq \omega_a \leq 10^{19.8}\,s^{-1}$ for positively charged fullerenes between $N = 42$ and 82.

In [82] Lifshitz and co-workers suggested a value of $\omega_a \approx 2 \times 10^{19}\,s^{-1}$ for C_{60}^+, based on data on metastable decay, in fair agreement with the values here and in [13,14]. A similar value for the frequency factor ($2 \times 10^{19}\,s^{-1}$) was used to successfully simulate the metastable decay of positive fullerenes in the ELISA storage ring [76] for a range of fullerene sizes similar to the above. The problem with the broad energy distributions which would give a powerlaw decay with no characteristic time was handled naturally by the radiative cooling which truncated the decay after several tens of microseconds. Modelling the radiative cooling, the temperature was extracted and converted to a dissociation energy, using an Arrhenius expression with the above frequency factor.

The important point here is that the data for $N = 62$–70 were compared with thermo-chemical data on the binding energies of C_{60} and C_{70}. The standard enthalpies of combustion of C_{60} and C_{70} have been determined by microcalorimetry (see [88] and references therein). These data provide a check of the absolute values of the dissociation energies. Consider the reaction:

$$C_{70}^+ \rightarrow C_{60}^+ + 5C_2. \quad (28)$$

The reaction enthalpy is given by the relevant gas-phase heats of formation ΔH_f deduced from measurements on the neutral species in thermodynamic equilibrium, with a small correction based on the ionization energies of C_{70} and C_{60} as explained in Section 2,

$$\Delta H_f(C_{70}, g) - \Delta H_f(C_{60}, g) - 5\Delta H_f(C_2, g) + \Phi_{60} - \Phi_{70} \approx \sum_{n=62}^{70} D_N^+. \quad (29)$$

This relation is not exact because it ignores the change in thermal energies between reactant and products, and the work term $p\Delta V$. However, a rough estimate [89] based on the equipartition theorem shows that this correction is less than the uncertainty of the average value of the left-hand-side, 41.0 ± 0.6 eV which was derived from a large number of published data [51]. This value is in excellent agreement with the sum of dissociation energies deduced from the ELISA data, 40.4 ± 0.8 eV [76]. The agreement suggests that the value assumed for the Arrhenius factor, for $N = 62$–70, was approximately correct.

8. Electron temperatures

Electron energy spectra provide very important information on the temperature of fullerenes undergoing thermal electron emission. These data allow one to compare the line in the (ω_a, D)-plane defined by Eq. (9) for C_2 emission with temperatures extracted from electron emission, i.e., from a different process and potentially different temperature. Likewise, it will be possible to test the hypothesis that C_2 emission is the dominant channel in decay of neutrals.

The thermal electron emission rate constant and the kinetic energy distribution is discussed in Appendix B. It is shown that the electron energy distributions are strongly influenced by the Coulomb potential and that they can be described by

quasi-Boltzmann distributions:

$$P(\varepsilon) \propto (\varepsilon + 4.1\,\mathrm{eV})\mathrm{e}^{-\varepsilon/k_B T_+}. \quad (30)$$

provided the electron sticking coefficient is unity. This is in good agreement with the experimentally measured electron kinetic energy distributions of Ding et al. [90], who fitted the temperature to $k_B T_f = 0.32 \pm 0.05$ eV, or $T_f = 3700 \pm 600$ K. No sign of a reverse activation barrier was seen.

A later and more detailed study of the thermal electron spectrum was made by Bordas et al. and gave a temperature of $k_B T_f = 3390 \pm 100$ K for decay between 1 μs and 1.1 μs after laser excitation [23]. With the assumption that the C_2 evaporation rate determines the highest temperature in the ensemble, this result provides an independent constraint on the possible values of D and ω_a as follows. The measured temperature is the product temperature for the electron emission process, $T_f(\Phi)$. It is related to the parent temperature as explained in Section 2.

With $k_a \simeq 1/(1\,\mu\mathrm{s})$ we have the emission temperature for C_2 decay:

$$T_e = T_m - \frac{D}{2c_m} = \frac{D}{k_B \ln(\omega_a 1\,\mu\mathrm{s})} \Rightarrow T_m = D\left(\frac{1}{k_B \ln(\omega_a 1\,\mu\mathrm{s})} + \frac{1}{2c_m}\right). \quad (31)$$

The measured temperature is found as $T_f = T_m - \Phi/c_m$. This can be solved for D which gives:

$$D = k_B \ln(w_a 1\,\mu\mathrm{s}) \frac{T_f(\Phi) + (\Phi/c_m)}{1 + (k_B \ln(\omega_a 1\,\mu\mathrm{s})/2c_m)}. \quad (32)$$

This result is independent of the detailed value of the frequency factor for electron emission, although it of course requires that it is not so high that electron emission dominates over C_2 emission.

Eq. (32) defines a curve in the (D, $\ln(\omega_a)$)-plane which is close to a straight line. The relative correction in the denominator is about 10%. The curve is plotted in Fig. 1. With the scatter in the nine points for C_2 emission and the nearly same slope on the line, it effectively does not add a new constraint to the possible values of D, ω_a. It does, however, confirm the previous analysis for the C_2 emission.

The measured temperature can also be used to determine an approximate value of the frequency factor for electron emission, when combined with data on the electron yield. If the limit of $2.6 \pm 1.1\%$ on the total electron yield from [65] is used, we have that $k_e \approx 0.026 k_a$, and hence

$$\frac{1}{t} = k_a + k_e = \left(\frac{1}{0.026} + 1\right) k_e = \omega_e \mathrm{e}^{\frac{-\Phi/k_B}{T_d + (\Phi/2c_m)}} \Rightarrow \omega_e = \frac{1}{39\,\mu\mathrm{s}} \mathrm{e}^{\frac{\Phi/k_B}{T_d + (\Phi/2c_m)}}. \quad (33)$$

where $t = 1\,\mu$s and $c_m = 173\,k_B$. This gives the value $\omega_e = 8.3 \times 10^{14}\,\mathrm{s}^{-1}$ with an errorbar of a factor of 2 to each side from the 100 K uncertainty on the temperature [23]. If all decay proceeds via electron emission, contrary to our expectations, the frequency factor increases to $3.1 \times 10^{16}\,\mathrm{s}^{-1}$ which must be considered an upper limit. For comparison, the frequency factor used in [24] to fit coincidence experiments was about $2.5 \times 10^{15}\,\mathrm{s}^{-1}$, i.e., a factor of 10 below the upper limit and a factor of 3 different from our estimate. In contrast, the integrated theoretical electron emission rate constant derived in Appendix B is a factor of 25 greater. There may be a number of reasons for the discrepancy. One possibility is that the degeneracy factor of 10 is overestimated, another that the sticking coefficient is less than unity. We do not expect this explanation to provide the answer, because neutral C_{60} has been found to capture low energy electrons with a sticking coefficient of typically 1/2, albeit with a dip around 0.4 eV [91]. A sticking factor of 1/2 would reduce the rate constant correspondingly. We expect that both charge state and temperature will favour sticking to hot cations, relative to cold and neutral molecules. Another possible explanation for the reduced rate constant could be that the electron yield is higher than the number given, but this can only explain a minor part of the difference, as can be seen from the above estimates.

9. Coincidence experiments

The analysis of the powerlaw decay in [64] demonstrated the possibility of extracting dissociation energies without any knowledge of the frequency factor. The downside of this is that the experiments are obviously then not sensitive to the value of this parameter.

A new development occurred when the Aarhus group embarked on an ambitious experiment in which electron emission and ion formation from multiphoton-excited C_{60} was measured in coincidence. This way the formation of C_{60}^+ and C_{58}^+ (formed from excited C_{58} fragments) could be monitored separately, as a function of time [24]. Using a dielectric model to estimate the radiative cooling, and the size distribution of the fragment ions to estimate the initial energy distribution $g(E)$, it was found that the Arrhenius factor ω_a for C_2 loss from C_{60} exceeds that of C_{58} by more than two orders of magnitude, while the Arrhenius factor of C_{70} exceeds that of C_{58} by one order of magnitude [53]. The increased precision caused by the coincidence technique made the determination of the value of p much more precise than previously. Combined with the fact that the electron yield from C_{60} was consistent with the one found in [65] and that electron emission therefore was confirmed as a minority channel allowed a precise determination of the dissociation energy of C_{60} to 10.6 eV [24,53], of C_{70} to 9.7 eV [53], and of C_{76} to 8.2 eV [92], with uncertainties of 0.3 eV in all three cases. The value for C_{60} is plotted in Fig. 1 as horizontal hatched area with a vertical height indicating the $\pm 1\sigma$ uncertainties.

The frequency factors are not determined directly in these experiments, but the ratios $\omega_{60}/\omega_{58} \approx 100$, $\omega_{70}/\omega_{68} \approx 10$ and $\omega_{76}/\omega_{74} \approx 1$ can be extracted from the data. Absolute values were calculated with an assumed frequency factor for electron emission. As we have seen, the values chosen is close to the one derived from the electron energy spectra data, and furthermore not extremely far from the theoretically calculated value. We therefore have some confidence also in the absolute values which are $\omega_{60} = 2.3 \times 10^{21}\,\mathrm{s}^{-1}$, $\omega_{70} = 1.7 \times 10^{20}\,\mathrm{s}^{-1}$ and $\omega_{76} = 1.0 \times 10^{19}\,\mathrm{s}^{-1}$.

10. Theoretical estimate of the frequency factor

Earlier attempts to calculate the frequency factor can be found in [28,57,85]. The frequency factor is not given explicitly in [57], but the rate constant is on the order of $10^5\ s^{-1}$ at $E = 50$ eV for an activation energy of 7 eV. With a temperature of 3890 K at this energy, the frequency factor would be about $10^{14}\ s^{-1}$, depending on the precise values of the frequencies used. In [28] a semiempirical expression by Klots is used, along with two other expressions which give rate constants that agree within an order of magnitude and a factor of 3–4 within that given in [57], and thus significantly below any value presently considered. In [85] the frequency factor was calculated with a slightly modified version of another theory of Klots' [35], which incorporates some of the features of the detailed balance equation given below. The result of $8 \times 10^{20}\ s^{-1}$ was considered an upper limit. A number of the contributions included in the derivation below were left out but a channel degeneracy was included, corresponding to a factor which counted the possible number of carbon atom combinations that can lead to evaporation. This was taken to be equal to the number of surface atoms, i.e., 60. This constitutes a double counting since the factor Q_{surf} already included the surface area. On the other hand, the dependence on the mass, Planck's constant and the rotational level density of the C_2 are represented correctly, and the result is much closer to the results in this paper than any previous attempts.

The detailed balance rate constant is given by [34,74]:

$$k_a\,\mathrm{d}\varepsilon = \frac{m_2\sigma\varepsilon}{\pi^2\hbar^3}\frac{\sum \rho_{N-2}(E-D-\varepsilon-\varepsilon')\rho_2(\varepsilon')}{\rho_N(E)}\,\mathrm{d}\varepsilon, \tag{34}$$

where m_2 is the reduced mass of the carbon dimer and the product molecule and will be approximated by the dimer mass, σ the capture cross section for the inverse process, $C_{N-2} + C_2 \rightarrow C_N$, ε the kinetic energy released in the evaporation process, E the excitation energy of the parent, D the dissociation energy, and the ρ's are the level densities of the molecules indicated by the subscript. The sum in the numerator is over all partitions of energy on the degrees of freedom of the two products. These include the vibrational, rotational and electronic degrees of freedom for both C_{N-2} and C_2. In addition, isomers may contribute to the state counting. Ideally, one should also take symmetry factors into account, but we will only include these for C_2. The translational degrees of freedom are already accounted for in Eq. (34). The cross section is energy dependent as seen in the KER distributions and discussed elsewhere. This is analogous to the expression for electron emission given in Appendix B but differs from this in important details because of the nature of the emitted particle.

The energy of the product is predominantly carried by the vibrational degrees of freedom of the large product molecule. There are $3N-12$ of those, compared with the one vibrational and two rotational degrees of freedom for the C_2, the three rotational degrees of freedom of the C_{N-2}, in addition to some electronic excitations, etc. We will therefore calculate the contribution to the rate constant from all degrees of freedom other than the vibrational in the canonical ensemble with the temperature given by the product temperature, in complete analogy to the procedure used for the KER and also used in [93] for the electronic degrees of freedom. Specifically, the partition of energy between one degree of freedom with level density ρ' and the vibrational degrees of freedom with level density ρ_v gives:

$$\sum \rho_v(E-\varepsilon')\rho'(\varepsilon') \approx \sum \rho_v(E)\mathrm{e}^{-\varepsilon'/k_BT_f}\rho'(\varepsilon')$$
$$= \rho_v(E)\sum \mathrm{e}^{-\varepsilon'/k_BT_f}\rho'(\varepsilon') = \rho_v(E)Z', \tag{35}$$

where Z' is the canonical partition function of the primed degree of freedom at temperature T_f.

This simplifies the expression Eq. (34) significantly because most contributions factor out. The rate constants become:

$$k_a\,\mathrm{d}\varepsilon = \frac{m_2\sigma\varepsilon}{\pi^2\hbar^3}Z_2(T_f)\frac{\rho_{N-2}(E-D-\varepsilon)}{\rho_N(E)}\,\mathrm{d}\varepsilon, \tag{36}$$

where $Z_2(T_f)$ is the canonical partition function of the carbon dimer at T_f. The isomer count and electronic degrees of freedom of C_{N-2} and C_N are included in $\rho_{N-2}(E)$ and $\rho_N(E)$. Neither the translational energy nor the rotational degrees of freedom of C_{N-2} appear in Eq. (36). This reflects the fact that both of these types of degrees of freedom have a conservation law associated with them. The unrestricted summation over states of both C_2 and C_{N-2} which involves a total of 6(vib) + 6(rot) degrees of freedom therefore reduces to a summation over 3(vib) + 3(rot) degrees of freedom. For the translational degrees of freedom this result is already implemented in Eq. (34) where the translational energy of C_{N-2} does not appear and the reduction of degrees of freedom has the sole effect of replacing the C_2 mass with the reduced mass. Quantitatively this effect is a relative correction of order m_2/m_{N-2}. For the rotations, the effect of an exact (classical) angular momentum conservation is numerically similar [77]. Physically, this can be understood as the ability of C_{N-2} to absorb the angular momentum of the evaporated C_2. For the emission of a point particle the relative correction to the rate constant from angular momentum conservation is found to be on the order of $4E_r/Nk_BT$ if the moments of inertia of product and precursor scale as N^2 (Eq. (21) in [77]). Here E_r is the rotational energy of the precursor. This correction will be ignored.

The thermal properties of C_2 can be calculated with the spectroscopic data available [94]. The most important electronic states are the $^1\sum_g^+$ ground state with a vibrational frequency of $1855\ \mathrm{cm}^{-1}$ and a rotational constant of $1.82\ \mathrm{cm}^{-1}$, and the first excited, $^3\Pi_u$, state at $716\ \mathrm{cm}^{-1}$ with a vibrational frequency of $1641\ \mathrm{cm}^{-1}$ and a rotational constant of $1.63\ \mathrm{cm}^{-1}$. In the calculations the seven lowest electronic states were used, up to an energy of $3.4 \times 10^4\ \mathrm{cm}^{-1}$. The symmetry factors, which are either 1 or 2 depending on the symmetry of the electronic configuration and the value of the vibrational quantum number, have also been included. The presence of low lying electronic excitations means that the partition function does not factor into separate rotational and vibrational contributions. The total contribution is calculated as:

$$Z(\mathrm{C}_2) = \sum_{i=0}^{6} g_i \frac{T}{2B_i}(1 + s + (2-s)\mathrm{e}^{-\hbar\omega_{v,i}/k_BT})$$
$$\times (1 - \mathrm{e}^{-2\hbar\omega_{v,i}/k_BT})^{-1} \tag{37}$$

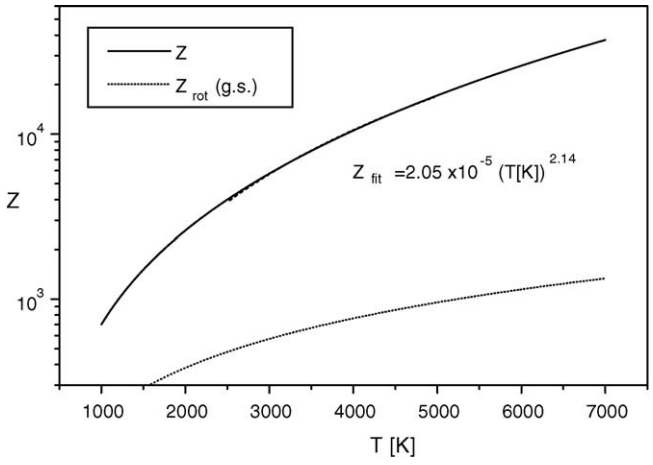

Fig. 2. The electronic–vibrational–rotational partition function of C_2 vs. temperature calculated as described in the text. Also shown is the rotational partition function of the vibronic ground state. The fit with the function described in the text is also shown, but is hardly discernible.

and shown in Fig. 2. The subscript i refers to the electronic state, the $w'_{v,i}$s are the vibrational frequencies, B_i the rotational constants, and g_i the spin degeneracy, 1 or 3. The value of s is 1 if the state is ungerade and 0 if gerade. The main contribution comes from the rotational partition functions but the contribution from vibronic excitations is not negligible. At $T = 3500$ K the ratio of the two is 11.8. The curve fits well the expression:

$$Z(C_2) = 2.05 \times 10^{-4}(T\,[\mathrm{K}])^{2.14} \tag{38}$$

between $T = 2500$ K and 5000 K.

The factors involving the cross section in Eq. (36) are calculated with an integration over ε to give:

$$\frac{m_2}{\pi^2\hbar^3}\int_0^\infty \mathrm{e}^{\varepsilon/k_BT_f}\sigma\varepsilon\,\mathrm{d}\varepsilon. \tag{39}$$

There is no experimental measurement of the cross section. We will therefore need to infer by other means. The most significant experimental evidences are the kinetic energy release distributions discussed elsewhere in the paper. They show quite unambiguously that there is no activation barrier for the attachment of a C_2 to a fullerene at elevated temperatures. This suggests, but does not guarantee that the cross section is not hindered by steric factors. Corroborative evidence for this is the shape of the energy distributions. They are consistent with a cross section strongly influenced by the polarizabilities of the species, with an enhanced low energy component. The lower limit of this cross section is the geometric one, $\sigma = \pi r_0^2$. An increased attraction at low fragment energies increases the cross section which ultimately becomes the Langevin cross section. When the polarization energy at the surface of the molecules is equal to the temperature, the integrated cross section in Eq. (39) is $1.9\pi r_0^2(k_BT_f)^2$ with the cross section in [77]. We will use the factor 1.5 instead of 1.9, for the cross section at $T_f = 3500$ K. The temperature dependence will be set to $T_f^{1.6}$, based on a fit of the numerical solution of Eq. (39). This gives an integrated cross section of:

$$\int_0^\infty \mathrm{e}^{\varepsilon/k_BT_f}\sigma\varepsilon\,\mathrm{d}\varepsilon \approx 1.5\pi r_0^2(k_B\,3500\,\mathrm{K})^2\left(\frac{T_f}{3500\,\mathrm{K}}\right)^{1.6}. \tag{40}$$

Including the remaining factors in Eq. (39) gives the factor:

$$\frac{m_2}{\pi^2\hbar^3}\int_0^\infty \mathrm{e}^{\varepsilon/k_BT_f}\sigma\varepsilon\,\mathrm{d}\varepsilon \approx 4.64\times10^{18}\left(\frac{T_f}{3500\,\mathrm{K}}\right)^{1.6}\mathrm{s}^{-1}$$
$$= 9.91\times10^{12}(T_f\,[\mathrm{K}])^{1.6}\,\mathrm{s}^{-1}. \tag{41}$$

The calculated value is somewhat higher than otherwise expected for clusters, mainly due to the fact that the temperature, which enters the expression squared, is higher for fullerenes than for most clusters due to the higher dissociation energy. The specific polarizability used and the power 1.6 does not change this conclusion. A higher polarizability gives a power closer to 1.5 but increases the dimensionless prefactor more than the corresponding reduction in temperature. The value must have some size dependence because the radius of the fullerenes is size dependent as well as their polarizabilities. The change is only serious if the C_N polarizabilities change significantly upwards and this possibility will be ignored in the following.

Isomers contribute to the level density of the motion of the nuclei. The precise degree to which they do so will depend on which isomers can be reached as a result of the fragmentation process and which are present in the ensemble of parent molecules. In the simplest picture every isomer contributes to the level density with a term which is identical to the ground state contribution, apart from a Boltzmann factor which accounts for the difference in energy relative to the ground state isomer. This requires that the vibrational level density of the isomer is the same as that of the ground state isomer. Calculations at different levels of theory have shown that the fullerene isomers of C_{60} have only positive vibrational frequencies and are therefore local points of stability (see [95] and references therein). Geometric structures calculated on the basis of topology can therefore be expected to represent true metastable isomers also for other fullerenes.

The rate of interconversion is another important issue. If different isomers are effectively prevented from converting to each other during the time of the experiment because of a high barrier for the process, they will not appear as terms in the level density of the precursor. In that case the rate constants should rather be summed over individual isomer species. Similarly, the product level density can only include the isomers that can be reached from the precursor state. The conversion rates for C_{60} have been investigated in [95] where it was found that the time to reach equilibrium through seven Stone–Wales rearrangements could be as long as milliseconds at excitation energies of 30–35 eV. At 54 eV the equilibration time was 100 ns, i.e., at the lower end of the experimental timescale relevant in this work. A further reduction in timescale must be expected if more channels open with the inclusion of non-classical fullerenes, involving heptagons and squares [96].

At the present level of our knowledge it is not possible to rigorously quantify the effect of isomers on the rate con-

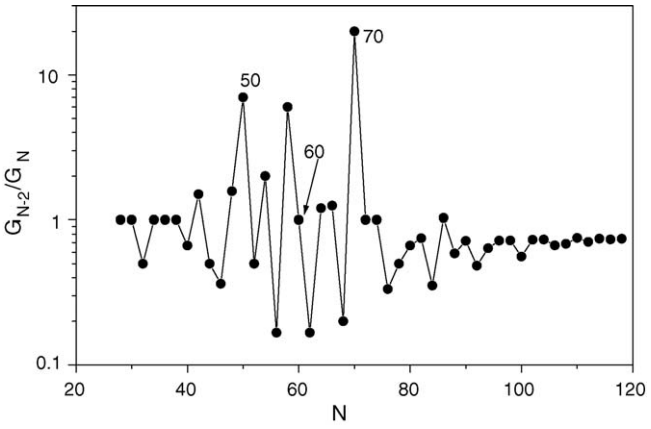

Fig. 3. The ratio of the ground state isomer degeneracies of C_{N-2} and C_N. This factor enters the rate constant as described in the text.

stant, but based on the above remarks we find it reasonable to include the number of lowest energy isomers for both the precursor and product in the rate constant. The number is found for each fullerene as the number of isomers with the lowest number of pentagon adjacencies, since each additional pentagon adjacency increases the energy by about 1 eV [97]. The number was calculated with the SPIRAL algorithm [98] and is denoted by G_N. The ratio G_{N-2}/G_N is plotted in Fig. 3 versus N. The values span two orders of magnitude, and deviate from unity most seriously between $N=50$ and 70. Some values are, e.g., $G_{48}/G_{50}=7$, $G_{58}/G_{60}=1$ and $G_{68}/G_{70}=20$. A calculation which includes all isomers weighted with a 1 eV adjacency penalty gives values that differ no more than a factor of 2 from the result shown in Fig. 3 for temperatures below 4000 K.

The electronic degrees of freedom contribute the ratio Z_{N-2}/Z_N to the rate constant. The same remarks concerning the equilibration times, as made above for the isomers, apply here, but the equilibration of the electronic degrees of freedom is expected to be faster than the ones involved in isomerization. The numerically most important cases involve closed shell molecules, primarily C_{60} and C_{70}, as either product or precursor. A calculation of all involved electronic states is beyond the ability of present computational methods, and we have calculated the ratio using the single particle approximation. The levels were calculated for C_{60} and C_{58} with density functional theory [99,100] for the decays $C_{60} \rightarrow C_{58} + C_2$ and $C_{60}^+ \rightarrow C_{58}^+ + C_2$. Very little of the neutral C_{60} shell closing is left in the ionized molecules, and the partition function ratio for the last process is close to unity: 1.18 at 3000 K, rising to 1.75 at 4000 K. We expect a similar behaviour for other molecules which do not have shell closings. For the neutral decay, the ratio is more constant, increasing from 8.4 to 10.3 between 3000 K and 4000 K. We will use the constant values 1.5 and 9 for the two cases. The value of 9 may also provide a reasonable approximation for the decay of neutral C_{70}. For decays involving other fullerenes, a value of 1 should give a reasonable approximation.

Combining the results of this section we have C_2 emission rate constants of:

$$k(E) = 2.03 \times 10^{10} (T\,[\mathrm{K}])^{3.74}\,\mathrm{s}^{-1}\,\frac{G_{N-2}}{G_N}\,\frac{Z_{el,N-2}}{Z_{el,N}} \times \frac{\rho_{N-2}(E-D)}{\rho_N(E)}, \tag{42}$$

where the ρ's are the vibrational level densities of the ground state molecules.

Before comparing this expression to the experimental determinations it is necessary to define more precisely the meaning of the frequency factor. The emission rate constant has been approximated with an Arrhenius expression in a number of places. In this expression the definition of the frequency factor is unambiguous if applied to a canonical ensemble. The situation is less obvious when the complete expression in Eq. (42) is used. Since neither the frequency factor nor the emission temperature are rigorously defined yet, their values can in principle be changed to arbitrary values by definition, while retaining the same rate constant. We will allow a temperature dependence of the frequency factor and in fact consider all factors external to the ratio of level densities as belonging to the frequency factor. This possibility is included explicitly in the analysis of the simulated electron emission data in Appendix A. Furthermore, we must demand that the finite heat bath correction commonly used to analyze experimental data will hold quantitatively. This is easiest accomplished if one defines the exponential in the Arrhenius expression as:

$$\frac{\rho_{N-2}(E-D)}{\rho_N(E)} \equiv c\left(\frac{\hbar\overline{\omega_v}}{T_f}\right)^6 \mathrm{e}^{-E_a/k_B T_e}. \tag{43}$$

The constant c is introduced for completeness and will turn out to be unity. The factor to the power 6 on the right hand side takes into account that 6 vibrational degrees of freedom have vanished from the molecule after C_2 evaporation. $\overline{\omega_v}$ is a geometric average of vibrational frequencies. The (high energy) vibrational level densities are:

$$\rho_N(E) = \frac{(E+E_{0,N})^{3N-7}}{(3N-7)!\prod_j \hbar\omega_{v,j}}, \tag{44}$$

where $E_{0,N}$ is the sum of vibrational zero point energies. Introducing this into Eq. (43), approximating $(3N-7)/(3N-13)$ with unity and cancelling terms, we get:

$$\left(\frac{E+E_{0,N-2}-D}{E+E_{0,N}}\right)^{3N-7} \equiv c\mathrm{e}^{-E_a/k_B T_e}. \tag{45}$$

With the parent temperature $k_B T_m = (E+E_{0,N})/(3N-7)$, the emission temperature $k_B T_e = k_B T_m - (D+E_{0,N}-E_{0,N-2})/2(3N-7)$, E_a becomes $D+E_{0,N}-E_{0,N-2}$. The appearance of the difference of zero point energies $E_{0,N}-E_{0,N-2}$, in the Arrhenius exponential is a fairly general feature if one wants to approximate ratios of level densities with an exponential. It is not an effect of the specific choice made in Eq. (43). Definitions of the exponential as $\rho_N(E-D)/\rho_N(E)$ or $\rho_{N-2}(E-D)/\rho_{N-2}(E)$ give the same result.

The above derivation has two consequences. One is that the experimentally determined dissociation energies should be reduced by $E_{0,N} - E_{0,N-2} = 6h\langle w_v\rangle$ for a comparison with theoretical values. With the frequencies calculated for C_{60} [99] this amounts to ca. 0.69 eV, which is within reach of experimental precision. The second consequence is that the theoretical frequency factor becomes:

$$\omega_a = 2.03 \times 10^{10}(T\,[\mathrm{K}])^{3.74}\,\mathrm{s}^{-1}\frac{G_{N-2}}{G_N}\frac{Z_{el,N-2}}{Z_{el,N}}\left(\frac{\hbar\overline{\omega_v}}{T_f}\right)^6. \tag{46}$$

If the geometric average $\hbar\overline{\omega_v} = 90\,\mathrm{meV}$ is used, the final result for the frequency factor is:

$$\omega_a = 2.03 \times 10^{10}(T\,[\mathrm{K}])^{3.74}\,\mathrm{s}^{-1}\frac{G_{N-2}}{G_N}\frac{Z_{el,N-2}}{Z_{el,N}}\left(\frac{\hbar\overline{\omega_v}}{T_f}\right)$$
$$= 2.6 \times 10^{28}(T\,[\mathrm{K}])^{-2.26}\,\mathrm{s}^{-1}\frac{G_{N-2}}{G_N}\frac{Z_{el,N-2}}{Z_{el,N}}. \tag{47}$$

For $T = 3500\,\mathrm{K}$ this equals:

$$\omega_a(3500\,\mathrm{K}) = 2.6 \times 10^{20}\,\mathrm{s}^{-1}\frac{G_{N-2}}{G_N}\frac{Z_{el,N-2}}{Z_{el,N}}. \tag{48}$$

The only value which can be directly compared with experiments is the one for neutral C_{60} which is $\omega_{60} = 2 \times 10^{21}\,\mathrm{s}^{-1}$. This compares very well with the experimental value of $\omega_{60} = 2.3 \times 10^{21}\,\mathrm{s}^{-1}$ [53] which was derived assuming a value $\omega_e = 1.0 \times 10^{15}\,\mathrm{s}^{-1}$ (for C_{60}, C_{70} and at a temperature of 4000 K). Note that the isomer factor (G_{58}/G_{60}) is unity for C_{60}. The perfect agreement is probably fortuitous. The electronic partition functions of the fullerenes involved in the other decays with experimentally derived frequency factors are not known. For ω_{70} the isomer degeneracy alone gives a factor 20 which gives a theoretical value which is a factor 30 above the experimental value. It does not seem likely that the entropy of the electronic degrees of freedom, not included in the estimate, can compensate for this factor. One would expect that this factor would actually increase this particular frequency factor. For C_{76} the isomer factor reduces the rate constant by a factor of three but it is still a factor of 9 higher than observed. The systematics of this, admittedly limited sample, suggests that the isomer degeneracy plays a smaller role than anticipated and that high frequency factors are correlated with high electronic stability. On the other hand, we now have theoretical estimates which either agree with or are moderately higher than experimental values. This appears to be a more satisfactory situation than the opposite.

11. Summary and conclusions

We have reviewed experiments on fullerenes with the purpose of extracting the frequency factors for C_2 emission. Several problems were identified with assignments made in the literature. Several robust experimental results were used to extract experimental values for, in particular, the frequency factor for C_{60}. These include powerlaw decays, metastable decay and coincidence measurements in electron emission experiments. The data give a consistent value for the C_{60} frequency around $10^{21}\,\mathrm{s}^{-1}$, much higher than usually expected for cluster decays or calculated with RRKM theory. Theoretical results were derived, based on the detailed balance formalism, and found to be in good agreement with the experimental results for C_{60}. The frequency factors for C_{70} and C_{76} were tentatively calculated and found to be overestimated in the theory by a factor which is significant but still with an error much smaller than that predicted by traditional reaction rate theory.

Acknowledgments

This work has been supported by VR and EU via with Research and Training Network HPRN-CT-2000-00026. Many valuable discussions on the subject and comments on the manuscript by J.U. Andersen are gratefully acknowledged.

Appendix A. Calculation of corrections to the powerlaw for the electron emission rate of C_{60}

The electron emission signal is given by:

$$I_e(t) = \int_0^\infty g(E)k_e\mathrm{e}^{-\{k_e+k_a)t}\,\mathrm{d}E, \tag{49}$$

with $g(E)$ the initial excitation energy distribution of the neutral C_{60}. In the simplest case [64] $g(E)$ was assumed constant, k_e was ignored in the exponential, and k_e, k_a were calculated with an Arrhenius expression without taking the finite heat bath correction into account. Here we will also leave out k_e in the exponential but otherwise generalize the expression by introducing energy dependences into g, ω_e and ω_a in addition to including the finite heat bath correction. The calculation will provide the corrections to p due to these effects.

We will assume that energy distributions and frequency factors depend on energy to some (small) power. This effectively mimics other types of dependences, because the energy range covered is rather small and it simplifies the calculation significantly. The notation used is:

$$g(E) \propto E^\alpha, \qquad \omega_e = \omega_e' E^\beta, \qquad \omega_a = \omega_a' E^\gamma, \tag{50}$$

where ω_e' and ω_a' are constants with proper dimensions to render the left hand sides of the definitions correct. The electron emission rate is then, to the approximation mentioned above,

$$I_e \propto \int_0^\infty E^\alpha k_e\mathrm{e}^{-(k_e+k_a)t}\,\mathrm{d}E, \tag{51}$$

where

$$k_e = \omega_e' E^\beta \mathrm{e}^{-\Phi/(k_BT-(k_B\Phi/2c_m))}, \tag{52}$$

and

$$k_a = \omega_a' E^\gamma \mathrm{e}^{-D/(k_BT-(k_BD/2c_m))}, \tag{53}$$

Without the energy dependences on the frequency factors and the finite heat bath correction the two rate constants are proportional, up to the power Φ/D, which made the integration of Eq. (51) very simple. Because the leading order term does not change,

we perform the same substitution to an integral over k_a here (the upper limit is an approximation which is justified in the light of the large frequency factor):

$$I_e \propto \int_0^\infty E(k_a)^\alpha k_e(k_a) \mathrm{e}^{-k_a t} \frac{\mathrm{d}E}{\mathrm{d}k_a}\, \mathrm{d}k_a. \tag{54}$$

The Jacobian is:

$$\frac{\mathrm{d}E}{\mathrm{d}k_a} = \frac{1}{k_a} \frac{1}{\frac{\gamma}{E} + \frac{D}{k_B c_m \left(T - \frac{D}{2c_m}\right)^2}} = \frac{1}{k_a} \frac{1}{\frac{\gamma}{E} + \frac{k_B (\ln(\omega_a/k_a))^2}{c_m D}}, \tag{55}$$

where E is to be understood as a function of k_a. We calculate $k_e(k_a)$ by solving Eq. (53) for T and inserting it in Eq. (52). From the resulting expression we extract the leading order factor $k_a^{\Phi/D}$. The result is:

$$k_e = k_a^{\Phi/D} \frac{\omega_e}{\omega_a^{\Phi/D}} \exp\left[\Phi \frac{k_B(D-\Phi)}{2c_m} \frac{1}{(D/\ln(\omega_a/k_a))((D/\ln(\omega_a/k_a)) + (k_B(D-\Phi)/2c_m))}\right] \tag{56}$$

Collecting these expressions, we have:

$$I_e \propto \int_0^\infty \mathrm{e}^{-k_a t} k_a^{\Phi/D-1} f\, \mathrm{d}k_a \tag{57}$$

where

$$f \equiv E(k_a)^\alpha \frac{\omega_e}{\omega_a^{\Phi/D}} \exp\left[\Phi \frac{k_B(D-\Phi)}{2c_m} \frac{1}{D/\ln(\omega_a/k_a)(D/\ln(\omega_a/k_a)) + (k_B(D-\Phi)/2c_m)}\right] \frac{1}{\gamma/E + k_B(\ln(\omega_a/k_a))^2/c_m D}. \tag{58}$$

The deviation of the factor f from a constant causes the correction to the value of p. Since Eq. (58) is a correction, it can be approximated without serious loss of precision. We have:

$$\frac{1}{\gamma/E + k_B(\ln(\omega_a/k_a))^2/c_m D} \approx \frac{c_m D}{k_B(\ln(\omega_a t/k_a t))^2}. \tag{59}$$

A factor t has been introduced on both the frequency factor and the rate constant in the ratio in the denominator. Similarly

$$E(k_a)^\alpha \frac{\omega_e}{\omega_a^{\Phi/D}} \propto E^{\alpha+\beta-\gamma\Phi/D} \propto (\ln(\omega_e t/k_a t))^{-(\alpha+\beta-\gamma\Phi/D)}, \tag{60}$$

where the approximate caloric curve $E \approx c_m T$ was used. A better approximation would include the finite heat bath correction and the offset in the caloric curve E_0, $E = c_m T - E_0$. The relative correction to the energy in Eq. (60) is approximately $(D/2 - E_0)/E$. For dissociation energies around 10 eV and excitation energies above a few tens of eV this almost vanishes because the terms both have absolute magnitudes of about 5 eV.

We will also approximate the denominator in Eq. (58) by leaving out the term $k_B(D-\Phi)/2c_m$, which is a 2–4% approximation on the calculated correction. Finally, we will set frequency factors appearing in logarithms to constants.

All factors in the correction depend on k_a in the form $\ln(k_a t)$, and we will use this to expand f to first order in this quantity before performing the integration. As the expansion point we will use $\langle k_a \rangle = \Phi/Dt$, calculated without the correction factor f in Eq. (57). This value can, for our purpose, be set equal to $1/t$, and the correction then becomes:

$$f \approx f(k_a t = 1) \exp\left(\ln(k_a t) \frac{\mathrm{d}\ln(f)}{\mathrm{d}\ln(k_a)}\bigg|_{k_a t = 1}\right). \tag{61}$$

With the above approximations we have that

$$f(k_a t = 1) = (\ln(\omega_a t))^{-(\alpha+\beta-\gamma\Phi/D+2)} \times \exp\left[\Phi \frac{k_B(D-\Phi)}{2c_m D^2} (\ln(\omega_a t))^2\right] \tag{62}$$

Eq. (57) then becomes:

$$I_e \propto \int_0^\infty \mathrm{e}^{-k_a t} k_a^{\Phi/D-1} f(k_a t = 1) \times \exp\left(\ln(k_a t) \frac{\mathrm{d}\ln(f)}{\mathrm{d}\ln(k_a)}\bigg|_{k_a t}\right) \mathrm{d}k_a \tag{63}$$

The last exponential is proportional to $k_a t$ to a constant power, δ say. After the substitution $x = k_a t$ we have:

$$I_e = f(k_a t = 1) t^{-\Phi/D} \int_0^\infty x^{\Phi/D-1} \mathrm{e}^{-x} x^\delta\, \mathrm{d}x \propto f(k_a t = 1) t^{-\Phi/D}. \tag{64}$$

A calculation of the double-logarithmic slope of this yield gives, together with Eq. (62), the power:

$$-p = \frac{\mathrm{d}\ln(I_e)}{\mathrm{d}\ln(t)} = -\frac{\alpha+\beta-\gamma\Phi/D+2}{\ln(\omega_a t)} - \frac{\Phi}{D} + \Phi \frac{k_B(D-\Phi)}{c_m D^2} \ln(\omega_a t). \tag{65}$$

The logarithmic curvature is the sum of the numerical values of the first and last term, divided by $\ln(\omega_a t)$, and is on the order of 10^{-3}, well within the 3% used as the criterion in the numerical simulations.

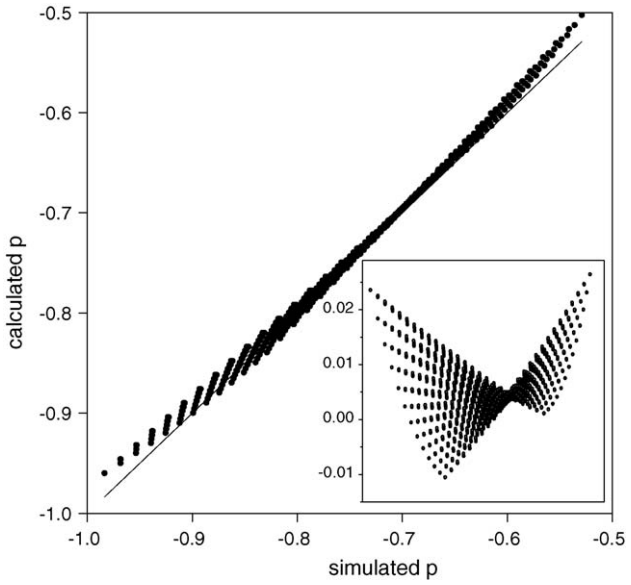

Fig. 4. Numerical calculation of the logarithmic slope of the electron yield vs. time as discussed in Appendix A. Points give individual values. The line has unit slope and zero intercept. The inset shows the difference between the calculated approximate slopes and those extracted from the simulations, with the same abscissa scale.

The values of β and γ depend on the precise functional form of the rate constants. If we use the kinetic energy release as a guideline, the values become $\beta = 1$ (electron spectra) and $\gamma = 1.5$ (C_2 emission). For α we can use the asymptotic value for a Gaussian laser beam [66], $\alpha = -1$.

For the sake of the argument we will assume $\ln(\omega_a t) = 33$ which was found in the metastable decay, and use $\Phi = 7.6$ and $D = 10.6$. This gives:

$$-p = -\frac{\Phi}{D} + 0.011, \tag{66}$$

or a 2% downward correction of the value of D extracted from the data. If we alternatively use the value -2 for γ, consistent with the theoretical estimate in Section 10, we get a more significant correction to the slope:

$$-p = -\frac{\Phi}{D} - 0.065, \tag{67}$$

which amounts to a 10% correction upwards for D.

In order to test the approximations made here we have calculated the value of p numerically for values of α, β and γ from -3 to 3 in steps of 0.5. The other parameters were $D = 10.6$ eV, $\Phi = 7.6$ eV, $\omega_e = 10^{15}\ s^{-1}$, and $\omega_a = 3 \times 10^{21}\ s^{-1}$, and the time interval [0.1 μs, 10 μs]. The result is shown in Fig. 4. The agreement between calculated and simulated values is generally reasonably good and particularly good around the experimentally relevant values between 0.6 and 0.7 where deviations between the approximate and the simulated values are 0.017 at the most.

In summary, we have seen that the corrections to the power in the powerlaw decay from energy dependences of the frequency factors and from the finite heat bath corrections have opposite sign. Depending on precisely how the frequency factors depend on the molecular excitation energy and on the laser profile, the terms may cancel or give rise to a correction.

Appendix B. The thermal electron emission rate constant of C_{60}

The thermionic emission rate constant, k_e, can be calculated with detailed balance, in analogy to the atomic emission rate constant, although somewhat simpler than the latter. The expression accounts both for the kinetic energy release of the electron and the total rate constant, and we will therefore calculate it in detail. The expression is analogous to neutron evaporation from a compound nucleus given by Weisskopf [74]:

$$k_e(E, \varepsilon)\mathrm{d}\varepsilon = g_e \frac{m_e \sigma(\varepsilon)}{\pi^2 \hbar^3} \varepsilon \frac{\rho_+(E - \Phi - \varepsilon)}{\rho_0(E)}\, \mathrm{d}\varepsilon \tag{68}$$

Here ε is the kinetic energy of the electron, m_e the mass of the electron (in principle the reduced mass of the channel), ρ_+, ρ_0 the level densities of the ion and the neutral molecule, respectively, and $\Phi = 7.6$ eV is the ionization potential. The factor $g_e = 2$ refers to the spin degeneracy of the electron. $\sigma(\varepsilon)$ is the energy dependent capture cross section for the electron in the inverse process. Both energy and momentum are conserved in this expression. We will disregard the complications due to the angular momentum of relative motion in the decay channel and the rotation of the molecule since the corrections are small for a large molecule.

The level densities in Eq. (68) are not restricted to purely nuclear degrees of freedom but include electronic excitations also. The spin degeneracy expresses this explicitly. It is convenient to factor these contributions from the molecules also. It can be done as shown in [93] in terms of the Helmholtz free energy, F, of the electronic subsystem ($\rho_{v,+}$ and $\rho_{v,0}$ denote the nuclear degrees of freedom for the cation and the neutral, respectively):

$$k_e(E, \varepsilon)\,\mathrm{d}\varepsilon = g_e \frac{m_e \sigma(\varepsilon)}{\pi^2 \hbar^3} \varepsilon \frac{\rho_{v,+}(E - \Phi - \varepsilon)}{\rho_{v,0}(E)}\, \mathrm{d}\varepsilon \times \exp\left(-\frac{F_+}{k_B T_+} + \frac{F_0}{k_B T_0}\right). \tag{69}$$

The two temperatures T_+ and T_0 are the microcanonical temperatures defined the usual way. Inclusion of the electronic degrees of freedom in this manner automatically takes into account the degeneracies of the electronic states of the molecule. Both, $k_B T_+$ and $k_B T_0$ are rather small compared to the band HOMO–LUMO gap in the molecule and for this reason one can approximate the exponential with the ratio of the degeneracies of the ion and neutral, i.e., the factor of g_+/g_0, if one includes the possible states with small splittings around the Fermi level. The neutral C_{60} molecule has a closed electronic shell with $g_0 = 1$. The factor for the positively charged molecules can be estimated from local density approximation calculations, with the obvious caveat that these calculations do not give energies of excited states and that calculations for neutral closed shell molecules do not apply to the ionic species, if not for anything else, then because of the Jahn–Teller splitting. Calculations by Scuseria [99] and Yabana [100] give either a 10-fold degeneracy for the positively charged molecule, or 10 states within an energy interval much smaller

than the expected temperature. We will therefore use a value of $g_+/g_0 = 10$ for the ratio.

The remaining physical content of Eq. (68) is contained in the cross section. We will use the classical capture cross section for an electron in a potential which is purely Coulombic at separations larger than the sphere radius and which corresponds to capture on a completely absorbing sphere. The capture cross section for such an electron–molecule collision is given by:

$$\sigma(\varepsilon) = \sigma_{\mathrm{geo}}(1 + (|V(r_0)|/\varepsilon)), \tag{70}$$

which can be calculated by conservation of energy and angular momentum. The potential $V(r_0)$ is the potential at the point of no return for the electron's radial motion. For a Coulomb potential and a value of $r_0 = 3.5$ Å corresponding to the radius of the C_{60} cage, $V(r_0) = -e^2/4\pi\varepsilon_0 r_0 = -4.1$ eV. The electron emission rate is then

$$k_e(E, \varepsilon)\,\mathrm{d}\varepsilon = \frac{g_+}{g_0} 2 \frac{m_e \pi r_0^2 (1 + |V(r_0)|/\varepsilon)}{\pi^2 \hbar^3} \varepsilon \frac{\rho_+(E - \Phi - \varepsilon)}{\rho_0(E)}\,\mathrm{d}\varepsilon. \tag{71}$$

Since $|V(r_0)|$ is substantially larger than the average kinetic energy, several eV compared to the ion temperature which is a fraction of an eV, the kinetic energy will essentially have a Boltzmann distribution with a small correction:

$$k_e(E, \varepsilon)\,\mathrm{d}\varepsilon \propto (\varepsilon + 4.1\,\mathrm{eV})\mathrm{e}^{-\varepsilon/k_B T_+}\mathrm{d}\varepsilon. \tag{72}$$

The integrated rate constant from Eq. (71) is:

$$k_e(E) = \frac{g_+}{g_0} \frac{2 m_e \pi r_0^2 (k_B^2 T_d^2 + |V(r_0)| k_B T_d)}{\pi^2 \hbar^3} \frac{\rho_+(E - \Phi - \varepsilon)}{\rho_0}$$
$$\approx 2.1 \times 10^{16}\,\mathrm{s}^{-1} \frac{\rho_+(E - \Phi - \varepsilon)}{\rho_0}, \tag{73}$$

using the temperatures measured by Bordas et al. [23].

References

[1] H.W. Kroto, J.R. Heath, S.C. O'Brien, R.F. Curl, R.E. Smalley, Nature 318 (1985) 162.
[2] R. Taylor, J.P. Hare, A.K. Abdul-Sada, H.W. Kroto, Chem. Commun. (1990) 1423.
[3] W. Krätschmer, L.D. Lamb, W.K. Fostiropoulos, D.R. Huffman, Nature 347 (1990) 354.
[4] M.S. Dresselhaus, G. Dresselhaus, P.C. Eklund, Science of Fullerenes and Carbon Nanotubes, Academic Press, New York, 1996.
[5] J.U. Andersen, C. Brink, P. Hvelplund, M.O. Larsson, B.B. Nielsen, H. Shen, Phys. Rev. Lett. 77 (1996) 3991.
[6] S.C. O'Brien, J.R. Heath, R.F. Curl, R.E. Smalley, J. Chem. Phys. 88 (1988) 220.
[7] P. Radi, T.L. Bunn, P.R. Kemper, M.E. Molchan, M.T. Bowers, J. Chem. Phys. 88 (1988) 2809.
[8] R. Mitzner, E.E.B. Campbell, J. Chem. Phys. 103 (1995) 2445.
[9] H. Hohmann, C. Callegari, S. Furrer, D. Grosenick, E.E.B. Campbell, I.V. Hertel, Phys. Rev. Lett. 73 (1994) 1919.
[10] A.A. Vostrikov, D.Y. Dubov, A.A. Agarkov, JETP Lett. 63 (1996) 963.
[11] S. Maruyama, M.Y. Lee, R.E. Haufler, Y. Chai, R.E. Smalley, Z. Phys. D 19 (1991) 409.
[12] E.E.B. Campbell, G. Ulmer, I.V. Hertel, Phys. Rev. Lett. 67 (1991) 1986.
[13] K. Hansen, E.E.B. Campbell, J. Chem. Phys. 104 (1996) 5012.
[14] M. Hedén, K. Hansen, F. Jonsson, E. Rönnow, A. Gromov, A. Taninaka, H. Shinohara, E.E.B. Campbell, J. Chem. Phys. 123 (2005) 044310.
[15] A.A. Agarkov, V.A. Galichin, S.V. Drozdov, D.Y. Dubov, A.A. Vostrikov, Eur. Phys. J. D 9 (1999) 331.
[16] P. Wurz, K.R. Lykke, J. Phys. Chem. 96 (1992) 10129.
[17] K.W. Kennedy, O. Echt, J. Phys. Chem. 97 (1993) 7088.
[18] M. Stuke, Y. Zhang, Phys. Rev. Lett. 75 (1995) 1235.
[19] G. von Helden, I. Holleman, A.J.A. van Roij, G.M.H. Knippels, A.F.G. van der Meer, G. Meijer, Phys. Rev. Lett. 81 (1998) 1825.
[20] E.E.B. Campbell, R.D. Levine, Ann. Rev. Phys. Chem. 51 (2000) 65.
[21] J.U. Andersen, E. Bonderup, K. Hansen, J. Phys. B 35 (2002) R1.
[22] O. Echt, S. Yao, R. Deng, K. Hansen, J. Phys. Chem. A 108 (2004) 6944.
[23] C. Bordas, B. Baguenard, B. Climen, M.A. Lebeault, F. Lépine, F. Pagliarulo, Eur. Phys. J. D 34 (2005) 151.
[24] S. Tomita, J.U. Andersen, K. Hansen, P. Hvelplund, Chem. Phys. Lett. 382 (2003) 120.
[25] J.U. Andersen, P. Hvelplund, S.B. Nielsen, U.V. Pedersen, S. Tomita, Phys. Rev. A 65 (2002) 053202.
[26] F. Lépine, B. Climen, F. Pagliarulo, B. Baguenard, M.A. Lebeault, C. Bordas, M. Hedén, Eur. Phys. J. D 24 (2003) 393.
[27] F. Lépine, C. Bordas, Phys. Rev. A 69 (2004) 053201.
[28] M. Foltin, M. Lezius, P. Scheier, T.D. Märk, J. Chem. Phys. 98 (1993) 9624.
[29] A.C. Jones, M.J. Dale, M.R. Banks, I. Gosney, P.R.R. Langridge-Smith, Mol. Phys. 80 (1993) 583.
[30] J.U. Andersen, E. Bonderup, Eur. Phys. J. D 11 (2000) 413.
[31] T. Baer, W.L. Hase, Unimolecular Reaction Dynamics, Oxford University Press, New York, 1996.
[32] J.U. Blatt, V.F. Weisskopf, Theoretical Nuclear Physics, Wiley, New York, 1952.
[33] P.A. Hervieux, D.H.E. Gross, Z. Phys. D 33 (1995) 295.
[34] K. Hansen, Philos. Mag. B 79 (1999) 1413.
[35] C.E. Klots, Z. Phys. D 20 (1991) 105.
[36] J.A. Zimmermann, J.R. Eyler, S.B.H. Bach, S.W. McElvany, J. Chem. Phys. 94 (1991) 3556.
[37] J. de Vries, H. Steger, B. Kamke, C. Menzel, B. Weisser, W. Kamke, I.V. Hertel, Chem. Phys. Lett. 188 (1992) 159.
[38] H. Steger, J. de Vries, B. Kamke, W. Kamke, T. Drewello, Chem. Phys. Lett. 194 (1992) 452.
[39] J.U. Andersen, E. Bonderup, K. Hansen, J. Chem. Phys. 114 (2001) 6518.
[40] J.U. Andersen, E. Bonderup, K. Hansen, P. Hvelplund, B. Liu, U.V. Pedersen, S. Tomita, Eur. Phys. J. D 24 (2003) 191.
[41] C. Yeretzian, K. Hansen, R.L. Whetten, Science 260 (1993) 652.
[42] T. Drewello, W. Krätschmer, M. Fieber-Erdmann, A. Ding, Int. J. Mass Spectrom. Ion Proc. 124 (1993) R1.
[43] A. Reinköster, S. Korica, B. Langer, G. Prümper, D. Rolles, J. Viefhaus, S. Cvejanovic, U. Becker, J. El. Spectrom. Rel. Phenom. 144 (2005) 151.
[44] R. Deng, O. Echt, Chem. Phys. Lett. 353 (2002) 11.
[45] Z. Wan, J.F. Christian, Y. Basir, S.L. Anderson, J. Chem. Phys. 99 (1993) 5858.
[46] Y. Basir, S.L. Anderson, J. Chem. Phys. 107 (1997) 8370.
[47] C.E. Klots, Z. Phys. D 21 (1991) 335.
[48] T. Sommer, T. Kruse, P. Roth, J. Phys. B 29 (1996) 4955.
[49] E. Kolodney, B. Tsipinyuk, A. Budrevich, J. Chem. Phys. 102 (1995) 9263.
[50] S. Matt, M. Sonderegger, R. David, O. Echt, P. Scheier, J. Laskin, C. Lifshitz, T.D. Märk, Chem. Phys. Lett. 303 (1999) 379.
[51] K. Gluch, S. Matt-Leubner, O. Echt, B. Concina, P. Scheier, T.D. Märk, J. Chem. Phys. 121 (2004) 2137.
[52] R. Wörgötter, B. Dünser, P. Scheier, T.D. Märk, M. Foltin, C.E. Klots, J. Laskin, C. Lifshitz, J. Chem. Phys. 104 (1996) 1225.
[53] B. Concina, S. Tomita, J.U. Andersen, P. Hvelplund, Eur. Phys. J. D 34 (2005) 191.
[54] P. Sandler, C. Lifshitz, C.E. Klots, Chem. Phys. Lett. 200 (1992) 445.

[55] J. Laskin, J.M. Behm, K.R. Lykke, C. Lifshitz, Chem. Phys. Lett. 252 (1996) 277.
[56] S. Matt, O. Echt, R. Wörgötter, P. Scheier, C.E. Klots, T.D. Märk, Int. J. Mass Spectrom. Ion Process. 167/168 (1997) 753.
[57] P. Weis, J. Rockenberger, R.D. Beck, M.M. Kappes, J. Chem. Phys. 104 (1996) 3629.
[58] C. Yeretzian, R.D. Beck, R.L. Whetten, Int. J. Mass Spectrom. Ion Process. 135 (1994) 79.
[59] T. Lill, H.G. Busmann, F. Lacher, I.V. Hertel, Chem. Phys. 193 (1995) 199.
[60] A. Bekkerman, B. Tsipinyuk, A. Budrevich, E. Kolodney, Int. J. Mass Spectrom. Ion Process. 167 (1997) 559.
[61] T. Fiegele, O. Echt, F. Biasioli, C. Mair, T.D. Märk, Chem. Phys. Lett. 316 (2000) 387.
[62] R. Deng, O. Echt, Int. J. Mass Spectrom. 233 (2004) 1.
[63] Z. Herman, Int. J. Mass Spectrom. 233 (2004) 361.
[64] K. Hansen, O. Echt, Phys. Rev. Lett. 78 (1997) 2337.
[65] R. Deng, O. Echt, J. Phys. Chem. A 102 (1998) 2533.
[66] K. Mehlig, K. Hansen, M. Hedén, A. Lassesson, A.V. Bulgakov, E.E.B. Campbell, J. Chem. Phys. 120 (2004) 4281.
[67] R.P. Radi, H. Ming-Teh, M.E. Rincon, P.R. Kemper, M.T. Bowers, Chem. Phys. Lett. 174 (1990) 223.
[68] C. Lifshitz, M. Iraqi, T. Peres, J.E. Fischer, Int. J. Mass Spectrom. Ion Process. 107 (1991) 565.
[69] P. Sandler, T. Peres, G. Weissman, C. Lifshitz, Ber. Bunsenges. Phys. Chem. 96 (1992) 1195.
[70] J. Laskin, T. Peres, A. Khong, H.A. Jimenez-Vazquez, R.J. Cross, M. Saunders, D.S. Bethune, M.S. DeVries, C. Lifshitz, Int. J. Mass Spectrom. 185–187 (1999) 61.
[71] T. Peres, B.P. Cao, H. Shinohara, C. Lifshitz, Int. J. Mass Spectrom. 228 (2003) 181.
[72] K. Gluch, S. Matt-Leubner, O. Echt, R. Deng, J.U. Andersen, P. Scheier, T.D. Märk, Chem. Phys. Lett. 385 (2004) 449.
[73] K. Gluch, S. Matt-Leubner, O. Echt, P. Scheier, T.D. Märk, J. Phys. Chem. A 108 (2004) 6990.
[74] V. Weisskopf, Phys. Rev. 52 (1937) 295.
[75] G.F. Bertsch, N. Oberhofer, S. Stringari, Z. Phys. D 20 (1991) 123.
[76] S. Tomita, J.U. Andersen, C. Gottrup, P. Hvelplund, U.V. Pedersen, Phys. Rev. Lett. 87 (2001) 073401.
[77] K. Hansen, Chem. Phys. Lett. 383 (2004) 270.
[78] J. Laskin, C. Weickhardt, C. Lifshitz, Int. J. Mass Spectrom. Ion Process. 161 (1997) L7.
[79] P. Fuentealba, Phys. Rev. A 58 (1998) 4232.
[80] A. Abdurahman, A. Shukla, G. Seifert, Phys. Rev. B 66 (2002) 155423.
[81] J. Laskin, C. Lifshitz, Chem. Phys. Lett. 277 (1997) 564.
[82] J. Laskin, B. Hadas, T.D. Märk, C. Lifshitz, Int. J. Mass Spectrom. 177 (1998) L9.
[83] K. Hansen, J.U. Andersen, P. Hvelplund, S.P. Møller, U.V. Pedersen, V.V. Petrunin, Phys. Rev. Lett. 87 (2001) 123401.
[84] F. Rohmund, M. Hedén, A.V. Bulgakov, E.E.B. Campbell, J. Chem. Phys. 115 (2001) 3068.
[85] C. Lifshitz, Int. J. Mass Spectrom. 198 (2000) 1.
[86] K. Hansen, U. Näher, Phys. Rev. A 60 (1999) 1240.
[87] V. Foltin, M. Foltin, S. Matt, P. Scheier, M. Becker, H. Deutsch, T.D. Märk, Chem. Phys. Lett. 289 (1998) 181.
[88] A. Rojas-Aguilara, J. Chem. Thermodyn. 34 (2002) 1729.
[89] B. Concina, K. Gluch, S. Matt-Leubner, O. Echt, P. Scheier, T.D. Märk, Chem. Phys. Lett. 407 (2005) 464.
[90] D. Ding, R.N. Compton, R.E. Haufler, C.E. Klots, J. Phys. Chem. 97 (1993) 2500.
[91] V. Kasperovich, G. Tikhonov, V.V. Kresin, Chem. Phys. Lett. 337 (2001) 55.
[92] B. Concina, S. Tomita, N. Takahashi, T. Kodama, S. Suzuki, K. Kikuchi, Y. Achiba, A. Gromov, J.U. Andersen, P. Hvelplund, Int. J. Mass Spectrom. 252 (2006) 96.
[93] K. Hansen, M. Manninen, J. Chem. Phys. 101 (1994) 10481.
[94] P.J. Linstrom, W.G. Mallard (Eds.), NIST Chemistry WebBook, NIST Standard Reference Database Number 69, June 2005. National Institute of Standards and Technology, Gaithersburg MD, 20899 (http://webbook.nist.gov).
[95] T.R. Walsh, D.J. Wales, J. Chem. Phys. 109 (1998) 6691.
[96] H. Hernández, P. Ordejón, H. Terrones, Phys. Rev. B 63 (2001) 193403.
[97] E.E.B. Campbell, P.W. Fowler, D. Mitchell, F. Zerbetto, Chem. Phys. Lett. 250 (1996) 544.
[98] P.W. Fowler, D.E. Manolopoulos, An Atlas of Fullerenes, Claredon Press, Oxford, 1995.
[99] G. Scuseria, Private communication.
[100] K. Yabana, Private communication.